Optical observation of the recharging processes of manganese ions in $YAlO_3$:Mn crystals under radiation and thermal treatment

2006 J. Phys.: Condens. Matter 18 5389

(http://iopscience.iop.org/0953-8984/18/23/011)

INSTITUTE OF PHYSICS PUBLISHING JOURNAL OF PHYSICS: CONDENSED MATTER

J. Phys.: Condens. Matter **18** (2006) 5389–5403 doi:10.1088/0953-8984/18/23/011

Optical observation of the recharging processes of manganese ions in $YAlO_3$:Mn crystals under radiation and thermal treatment

Ya Zhydachevskii[1], A Suchocki[2], D Sugak[3], A Luchechko[4], M Berkowski[2], S Warchol[5] and R Jakieła[2]

[1] Lviv Polytechnic National University, 12 Bandera, Lviv 79646, Ukraine
[2] Institute of Physics, Polish Academy of Sciences, 32/46 Aleja Lotnikow, Warsaw 02668, Poland
[3] Institute of Materials, SRC 'Carat', 202 Stryjska, Lviv 79031, Ukraine
[4] I Franko Lviv National University, 107 Tarnavsky, Lviv 79017, Ukraine
[5] Institute of Nuclear Chemistry and Technology, 16 Dorodna, Warsaw 03195, Poland

Received 1 December 2005
Published 26 May 2006
Online at stacks.iop.org/JPhysCM/18/5389

Abstract

Mn-doped $YAlO_3$ crystals have been characterized by means of optical absorption, photoluminescence, x-ray luminescence and thermoluminescence measurements. The influence of after-growth high-temperature thermal treatments of the crystals in oxidizing and reducing atmosphere as well as the effect of co-doping with Si^{4+} on the optical properties of the crystals have been studied. The recharging processes of manganese ions involving Mn^{3+}, Mn^{4+} and Mn^{5+} ions in octahedral (Al) positions, which take place under ionizing irradiation and thermal treatments, have been studied.

1. Introduction

Yttrium orthoaluminate crystals ($YAlO_3$) are known mainly as host material for solid-state lasers. Manganese-doped $YAlO_3$ crystals became of particular interest after it was shown that they have a high application potential for holographic recording and optical data storage [1–3] as well as for thermoluminescent dosimetry of ionizing radiation [4].

Holographic recording on $YAlO_3$:Mn crystals is accompanied by photocolouration caused by ionization of Mn^{4+} ions ($Mn^{4+} \rightarrow Mn^{5+} + e^-$) that occupy octahedral (Al) positions in the lattice [1, 2, 5].

Our previous thermoluminescence (TL) studies of $YAlO_3$:Mn crystals [6] have shown that besides ionization of Mn^{4+} ions, ionizing irradiation of the crystals also leads to recharging of Mn^{2+} ions (most likely the $Mn^{2+} \rightarrow Mn^{3+} + e^-$ ionization) that occupy the Y positions in the crystal [5]. The electrons released from both Mn^{2+} and Mn^{4+} ions are captured on deep traps available in the host. During warming up of the irradiated crystals from room temperature to about 650 K, the electrons are released from the traps and recombined on Mn ions. This process

is accompanied by the red and yellow–green TL emissions that correspond to the luminescence of the Mn^{4+} (transition $^2E \rightarrow {}^4A_2$) and Mn^{2+} (transition $^4T_1 \rightarrow {}^6A_1$) ions, respectively. The yellow–green TL emission with a maximum near 530 nm originating from Mn^{2+} ions has been used as a TL signal for detection of ionizing radiation [4].

The present work is a continuation of our previous studies [4, 6] and includes details on the growth of Mn-doped $YAlO_3$ crystals and their characterization by means of optical absorption, photoluminescence, x-ray luminescence and thermoluminescence measurements. In addition, the influence of post-growth high-temperature thermal treatments of the crystals in oxidizing and reducing atmosphere as well as the effect of co-doping with Si^{4+} on the properties of the crystals have been studied. The studies have been performed from the point of view of possible optimization of the crystal properties for the TL dosimetry application.

2. Experimental procedure

2.1. Crystal growth

Manganese-doped single crystals of $YAlO_3$ were grown by the Czochralski method in the Institute of Physics, Polish Academy of Sciences. The crystals were grown from the melt containing 4 mol% more yttrium than aluminium oxide in comparison with the stoichiometric composition. Such a composition of the melt was chosen taking into account our previous growth experiments for pure $YAlO_3$ crystals. Among three pure $YAlO_3$ crystals grown from melts of different compositions ((i) a stoichiometric one, (ii) 2 mol% more Y_2O_3 than Al_2O_3 and (iii) 4 mol% more Y_2O_3 than Al_2O_3) the third one, in spite of the red–brown colouration, was found to have the best structural quality. This is also in agreement with the results reported in [7]. The growth processes were carried out in an iridium crucible 40 mm in diameter at the pulling rate of 1–1.5 mm h^{-1} and a rotation rate of 20 rpm in pure nitrogen atmosphere. Manganese and silicon were added to the melt in the form of MnO_2 and SiO_2 at the expense of aluminium oxide. Good quality single crystals of 19 mm in diameter were grown using a seed oriented along the ⟨001⟩ crystallographic direction.

The following crystals have been studied in the present work: $YAlO_3$:Mn(0.1%); $YAlO_3$:Mn(0.2%) and $YAlO_3$:Mn(0.2%), Si(0.2%). The dopant concentration corresponds to the nominal concentration in the melt with respect to aluminium. The manganese and/or silicon concentration in the crystals was not measured directly. However, it was shown previously that manganese concentration in $YAlO_3$ can be 10–12 times lower than that in the melt [1]. The presence of silicon was confirmed by the SIMS technique. Owing to the small ionic radius of Si^{4+} ions (0.4 Å in octahedral coordination [8]), it can be assumed that Si^{4+} ions occupy Al positions in the crystal.

Unlike the previously studied $YAlO_3$:Mn(0.05% and 0.5%) crystals that were yellowish [1], the as-grown crystals studied here have an olive colour of different intensity. Besides the as-grown crystals, samples annealed in hydrogen flow or in air (both at temperature 1300 K for 1 h) were also studied.

2.2. Spectroscopic methods and experimental set-ups

Optical absorption of the crystals was measured using a Cary 5000 UV–vis–NIR spectrophotometer.

Irradiation with γ-rays was performed using an ^{60}Co source with a 1.6 kGy h^{-1} dose rate. An Innova 400 (Coherent) Ar^+ laser at $\lambda = 514.5$ nm was used for excitation in photoluminescence measurements as well as to produce photocolouration of the crystals.

An additional absorption that arises in the crystals after various treatments (irradiation or annealing) was determined as the difference between the optical absorption after and before the treatment.

In order to study the discolouration processes, a number of warming processes in air were performed with the step of 30 K until the crystal colour returned to the initial (unexposed) state. Each warming process lasted for 20 min at a certain temperature; after this the crystal was cooled down to room temperature, whereupon the optical absorption of the crystal was measured. In this way a number of absorption spectra, which correspond to intermediate states of crystal colouration between the exposed (coloured) state and completely discoloured state, were obtained.

The TL measurements were performed using a hand-made set-up equipped with a compact furnace and a Triax 320 (Jobin Yvon-Spex) monochromator with a CCD camera. The samples were heated from room temperature to 650 K with the rate of 0.4 K s^{-1}. Application of the monochromator with a CCD camera allowed us to separate the red and yellow–green TL emissions as well as to obtain spectra of TL emission during the experiments. The multimeter and the monochromator with CCD camera were interfaced by IEEE 488 (GPIB) to a PC where the experimental data were processed and stored. The same monochromator with CCD camera was also used for photoluminescence measurements. A Leybold cryogenerator with an LTC60 temperature controller was used for low-temperature (10–320 K) photoluminescence measurements.

The emission spectra at x-ray excitation were registered through a monochromator by a photomultiplier. The excitation was performed by a microfocus x-ray tube operated under a voltage of 45 kV with a current of 0.3 mA. The emission spectra were corrected for the dispersion of the monochromator and spectral response of the photomultiplier.

3. Experimental results and discussion

3.1. Characterization of as-grown crystals and crystals annealed in oxidizing/reducing atmosphere

The optical absorption spectra of the Mn-doped $YAlO_3$ crystals are presented in figure 1. As is seen from the figure, besides Mn^{4+} ions that are responsible for the absorption band centred at about 21 000 cm^{-1} (transition $^4A_2 \rightarrow {}^4T_2$ in Mn^{4+} ions [9]), Mn^{5+} ions are also present in the as-grown $YAlO_3$:Mn crystals and reveal themselves in absorption bands near 12 000, 15 000, 18 000 and ∼26 000 cm^{-1} (transitions $^3T_1(^3F) \rightarrow {}^3T_2(^3F)$, $^3T_1(^3F) \rightarrow {}^3T_1(^3P)$ and $^3T_1(^3F) \rightarrow {}^3A_2(^3F)$ in Mn^{5+} ions [10]). An intensive absorption in the UV region is caused by O–Mn charge transfer bands [10]. The presence of Mn^{5+} ions in the as-grown crystals is the reason for the olive colour of the crystals.

Our photoluminescence measurements also testify to the presence of Mn^{4+} ions in the as-grown $YAlO_3$:Mn crystals. The characteristic luminescence spectra of Mn^{4+} ions are shown in figure 2. Note that no photoluminescence of Mn^{3+} ions in the as-grown crystals was seen. The luminescence spectrum of Mn^{4+} ions consists of two sharp lines at 691.3 and 692.7 nm, which become apparent at low temperature as for most high-energy ones, and their vibronic sidebands. The lines at 691.3 and 692.7 nm have been attributed to *R* lines (transition $^2E \rightarrow {}^4A_2$) of Mn^{4+} ions [11].

The high-temperature annealing of as-grown $YAlO_3$:Mn crystals in a reducing atmosphere (hydrogen) removes practically completely the absorption at 12 000, 15 000 and 18 000 cm^{-1} (see figure 1). This means that such annealing reduces the number of Mn^{5+} ions present in the as-grown crystals, apparently by way of the $Mn^{5+} \rightarrow Mn^{4+}$ reaction, which is charge compensated by the loss of oxygen from the crystal.

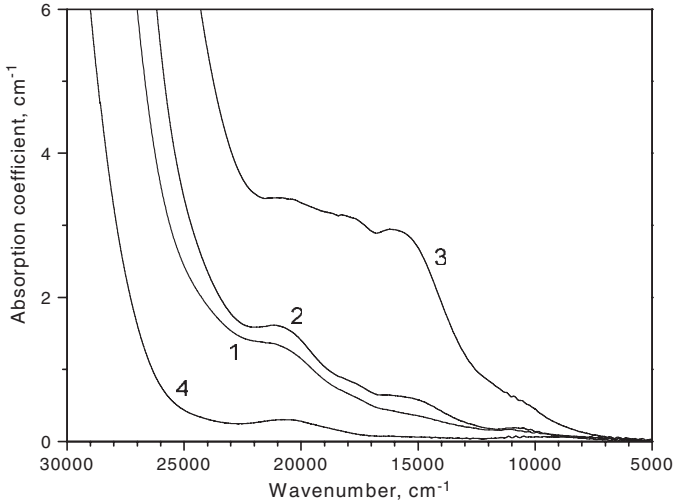

Figure 1. Non-polarized optical absorption spectra of $YAlO_3$:Mn crystals recorded at room temperature: 1—as-grown $YAlO_3$:Mn(0.1%) crystal; 2—as-grown $YAlO_3$:Mn(0.2%) crystal; 3—$YAlO_3$:Mn(0.2%) crystal annealed in air ($T = 1300$ K); 4—$YAlO_3$:Mn(0.2%) crystal annealed in hydrogen ($T = 1300$ K).

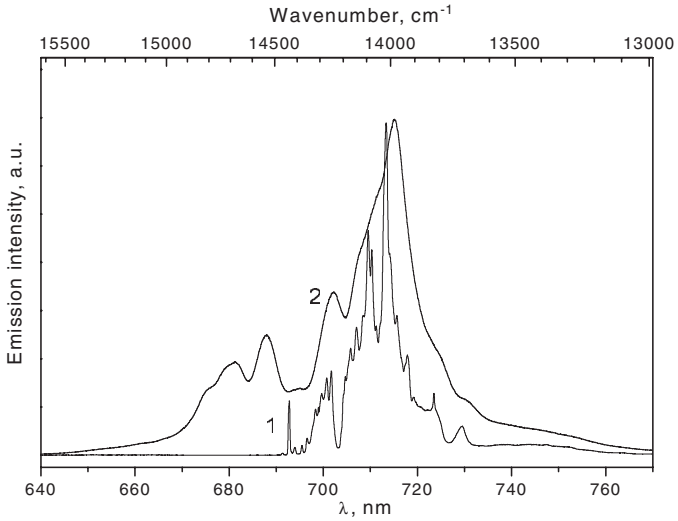

Figure 2. Photoluminescence spectra of the as-grown $YAlO_3$:Mn(0.2%) crystal using Ar^+-laser excitation ($\lambda = 514.5$ nm), recorded at temperature $T = 10$ K (1) and $T = 320$ K (2).

An increase of the Mn^{4+} ion concentration in the hydrogen annealed crystals has also been confirmed by x-ray luminescence measurements. As seen in figure 3, the red emission near 710 nm, which we correlate with Mn^{4+} ions, increases by a factor of 1.6 in the hydrogen annealed crystal in comparison with the as-grown crystal. One can speculate that the increase of the red emission near 710 nm (14 000 cm^{-1}) after hydrogen annealing is due to a decrease of the crystal absorption in this spectral region (see figure 1). Our calculations show that the decrease of reabsorption at 710 nm should result in the rise of red emission only by a factor

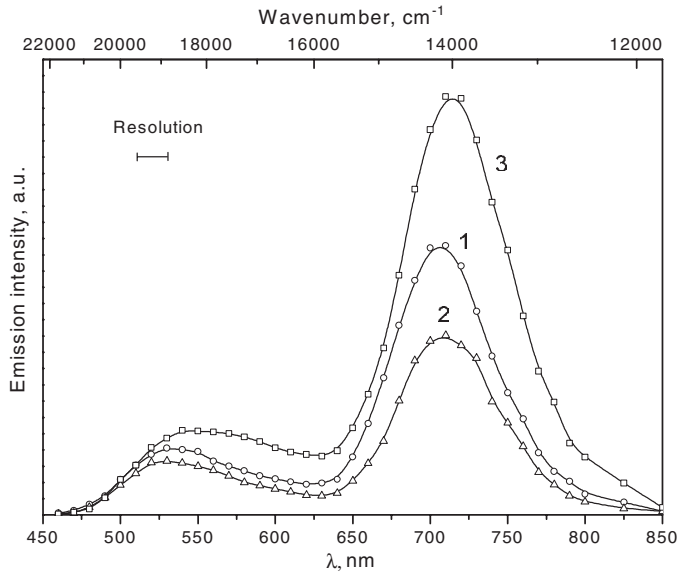

Figure 3. X-ray luminescence spectra of $YAlO_3$:Mn(0.2%) crystal: 1—as-grown; 2—air annealed; 3—hydrogen annealed.

of 1.03 in the experimental set-up used. This proves that the Mn^{4+} ion concentration indeed increases after hydrogen annealing, although a rise of the Mn^{4+} absorption band is not visible at first sight. It should be kept in mind, however, that the Mn^{4+} absorption band for the as-grown and air annealed crystals is superimposed on the absorption bands of Mn^{5+} ions.

We correlate another emission band peaked at about 530 nm observed under x-ray excitation with Mn^{2+} ions. This emission band also increases (by a factor of 1.3) in the hydrogen annealed crystals (see figure 3). In this case the increase expected for reduced reabsorption is 1.05. By analogy to Mn^{4+} ions, it could be deduced that hydrogen annealing increases the number of Mn^{2+} ions. According to this, we expect the presence of Mn^{3+} ions in Y positions in as-grown crystals and the $Mn^{3+} \rightarrow Mn^{2+}$ reduction reaction under hydrogen annealing. However, this remains only a supposition, because no evidence of Mn^{3+} ions in the as-grown crystals was obtained from our photoluminescence measurements, as mentioned above. Moreover, the yellow–green emission has a complex structure (see figures 3 and 4) and can involve some other emission bands not related to Mn^{2+} ions. Such emission can originate from defect centres as observed under UV excitation in [12]. Hence, the possibility that emitting centres other than Mn^{2+} ions give rise to the 500–600 nm emission at x-ray excitation cannot be excluded. Further studies of these effects are under way.

The high-temperature annealing of the crystals in oxidizing atmosphere (in air) has an inverse effect. It increases the number of Mn^{5+} ions, as evidenced by the increased absorption at 12 000, 15 000 and 18 000 cm^{-1} (see figure 1). Also, x-ray luminescence spectra show a reduction of the red emission from Mn^{4+} ions by a factor of 1.5 (a calculated factor due to changes in reabsorption is only 1.12) as compared with the as-grown crystal (see figure 3). Thus, the $Mn^{4+} \rightarrow Mn^{5+}$ reaction takes place under the oxidizing annealing of the crystals. Regarding the yellow–green emission near 530 nm, the observed reduction relative to the as-grown crystal (by a factor of 1.2) is commensurable with the calculated factor caused by changes in reabsorption in this spectral region.

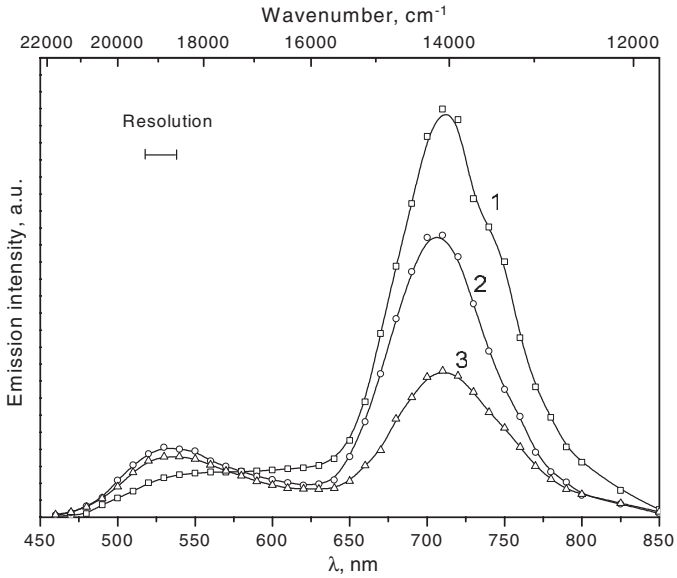

Figure 4. X-ray luminescence spectra of as-grown crystals: 1—$YAlO_3$:Mn(0.1%); 2—$YAlO_3$:Mn(0.2%); 3—$YAlO_3$:Mn(0.2%), Si(0.2%).

Comparing the x-ray luminescence spectra of the as-grown crystals of different compositions (see figure 4), namely the crystals of $YAlO_3$:Mn(0.1%), $YAlO_3$:Mn(0.2%) and $YAlO_3$:Mn(0.2%), Si(0.2%), the following observations can be made. The red emission from Mn^{4+} ions for the $YAlO_3$:Mn(0.2%) crystal is smaller than for the $YAlO_3$:Mn(0.1%) crystal, while the yellow–green emission from Mn^{2+} ions for the $YAlO_3$:Mn(0.2%) crystal is greater than for the $YAlO_3$:Mn(0.1%) crystal. This confirms indirectly the supposition mentioned in [1] that the incorporation of manganese in the $YAlO_3$ host is limited not only by its concentration in the melt. The intrinsic defects which provide the charge compensation for Mn^{4+} and Mn^{2+} ions are also an important factor. Another interesting observation is that co-doping with silicon practically does not change the intensity of the yellow–green emission from Mn^{2+} ions and at the same time reduces the emission intensity of Mn^{4+} ions by a half. The observed ratio of the yellow–green emission to the red emission at x-ray excitation is about 0.10; 0.25 and 0.42 in the as-grown crystals of $YAlO_3$:Mn(0.1%); $YAlO_3$:Mn(0.2%) and $YAlO_3$:Mn(0.2%), Si(0.2%), respectively.

3.2. Thermoluminescence after green laser illumination and ionizing irradiation

The TL glow curves of the $YAlO_3$:Mn(0.2%) crystal both as grown and previously annealed in reducing/oxidizing atmosphere after green laser illumination are presented in figure 5. The TL emission occurs only in the red spectral region and corresponds to the luminescence of Mn^{4+} ions. The TL glow curves contain three main peaks at 400, 450 and 560 K at the heating rate of 0.4 K s^{-1}, which is in agreement with the previously reported peaks at 360, 400 and 500 K at the 0.1 K s^{-1} heating rate [6]. As will be shown below, the colouration caused by the laser illumination is removed completely after the crystal is warmed up to $T = 650$ K, i.e., the crystal returns to the previous unexposed state.

It should be kept in mind that the intensity of the third TL peak (∼560 K) is strongly reduced (about two orders of magnitude) due to the thermal quenching of the Mn^{4+} ion

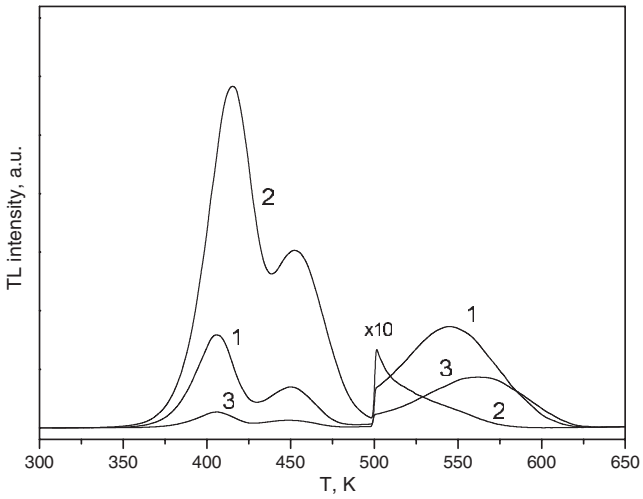

Figure 5. Thermoluminescence glow curves of $YAlO_3$:Mn(0.2%) crystal registered in the red spectral region after green laser ($\lambda = 514.5$ nm) illumination using 0.4 K s^{-1} heating rate: 1—as-grown crystal; 2—air annealed crystal; 3—hydrogen annealed crystal.

luminescence. The detailed photoluminescence studies of Mn^{4+} ions in $YAlO_3$ [11] show that the thermal quenching starts above $T = 420$ K. Thus, only 5% of the intensity is observed at $T = 500$ K. In fact, the thermal quenching of the emission intensity is the reason for the reduced value of the activation energy of the third TL peak determined in [6] by the initial rise method.

As can be seen in figure 5, the integral intensity of the first two TL peaks of the crystal previously annealed in air is a few times greater than in the as-grown crystal. Vice versa, the intensity of the first two TL peaks of the crystal previously annealed in hydrogen is a few times lower in comparison with the as-grown crystal. Owing to the strong thermal quenching of the third TL peak it is hard to compare its intensity in the as-grown and hydrogen annealed crystals. Nevertheless, a considerable reduction of the third TL peak for the crystal previously annealed in air is clearly visible.

The TL glow curves in red and yellow–green spectral regions after ionizing irradiation of various $YAlO_3$:Mn crystals are presented in figures 6 and 7. The TL glow curve in the red spectral region is similar to that after laser illumination. However, in the case of γ-irradiation the first two peaks are much more intense relative to the third peak. Similarly to the TL glow after laser illumination, the integral intensity of the first two peaks for the crystal previously annealed in air is greater in comparison with the as-grown crystal. Vice versa, the integral intensity of the first two peaks for the crystal previously annealed in hydrogen is smaller in comparison with the as-grown crystal (see figure 6).

The TL glow in the yellow–green spectral region after γ-irradiation reveals some peculiarities (see figure 7). In addition to the two TL peaks at 400 and 450 K that are also observed in the red spectral region, a peak at 380 K is observed. The peak is weak for as-grown crystals and crystals previously annealed in air. In contrast to the red TL emission, annealing in air reduces the intensity of the peaks at 400 and 450 K, while annealing in hydrogen leads to an increase of the integral intensity of the yellow–green emission, mainly due to the drastic growth of the peak at 380 K. In addition, a new peak at 490 K appears for the hydrogen annealed crystal.

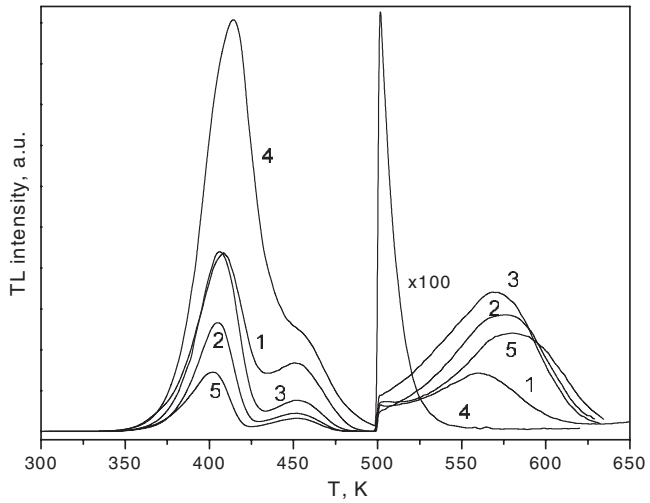

Figure 6. Thermoluminescence glow curves of $YAlO_3$:Mn crystals registered in the red spectral region after γ-irradiation (dose of 1 kGy) using 0.4 K s^{-1} heating rate: 1—as-grown $YAlO_3$:Mn(0.1%) crystal; 2—as-grown $YAlO_3$:Mn(0.2%), Si(0.2%) crystal; 3—as-grown $YAlO_3$:Mn(0.2%) crystal; 4—$YAlO_3$:Mn(0.2%) crystal annealed in air; 5—$YAlO_3$:Mn(0.2%) crystal annealed in hydrogen.

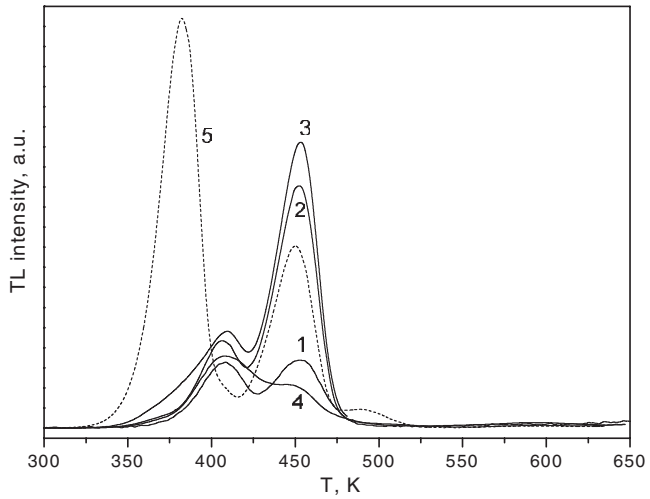

Figure 7. Thermoluminescence glow curves of $YAlO_3$:Mn crystals registered in the yellow–green spectral region after γ-irradiation (dose of 1 kGy) using 0.4 K s^{-1} heating rate: 1—as-grown $YAlO_3$:Mn(0.1%) crystal; 2—as-grown $YAlO_3$:Mn(0.2%), Si(0.2%) crystal; 3—as-grown $YAlO_3$:Mn(0.2%) crystal; 4—$YAlO_3$:Mn(0.2%) crystal annealed in air; 5—$YAlO_3$:Mn(0.2%) crystal annealed in hydrogen.

In order to convert the γ-irradiated crystals (in particular the as-grown and oxidized crystals) to the previous unexposed state, they should be warmed up to $T = 650$ K, similarly as in the case of laser illumination. On the other hand, the crystals previously annealed in hydrogen should be warmed up to $T = 850$ K in order to obtain the same effect, which will be shown below.

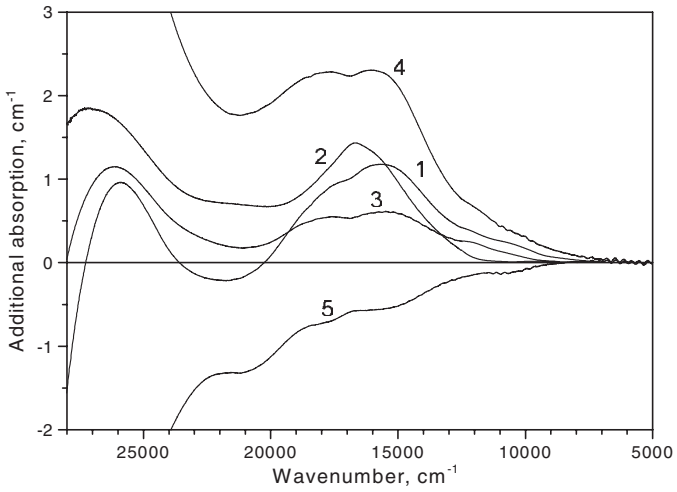

Figure 8. Additional absorption spectra of the $YAlO_3$:Mn(0.2%) crystals after laser ($\lambda = 514.5$ nm) illumination: 1—as-grown crystal; 2—crystal annealed in air; 3—crystal annealed in hydrogen. Additional absorption spectra of the $YAlO_3$:Mn(0.2%) crystal annealed in air (4) and the crystal annealed in hydrogen (5) both relative to the as-grown crystal.

3.3. Colouration and discolouration processes after green laser illumination

The green laser illumination of the studied $YAlO_3$:Mn crystals causes photocolouration that is shown in figure 8. Here we also present the additional absorption spectra caused by the oxidizing/reducing treatments relative to as-grown crystal. As can be seen, the laser illumination of both as-grown and reduced crystals gives rise to the absorption bands of Mn^{5+} ions (at 12 000, 15 000, 18 000 and probably 26 000 cm^{-1}), that agrees with the photoionization of Mn^{4+} ions. However, the induced absorption of Mn^{5+} ions in the hydrogen annealed crystal, at least at 20 000–10 000 cm^{-1}, is smaller than in the as-grown crystal. Since the same illumination dose was used, one can conclude that annealing in reducing atmosphere decreases the number of deep traps, which can capture electrons released in the $Mn^{4+} \rightarrow Mn^{5+} + e^-$ ionization process. This conclusion is in agreement with the smaller TL yield from Mn^{4+} ions observed in crystals annealed in a reducing atmosphere.

Laser illumination of the crystal previously annealed in air, which already contains a noticeable amount of stable Mn^{5+} ions in the host, causes additional colouration that noticeably differs from those observed in the as-grown and hydrogen annealed crystals. This additional colouration is characterized by a dominant absorption band peaked at about 16 500 cm^{-1} (curve 2 in figure 8).

The residual optical absorption that remains after warming processes as a function of temperature, hereafter called the discolouration kinetics, is presented in figure 9 for the laser illuminated $YAlO_3$:Mn crystals. As can be seen in the figure, the laser induced absorption bleaches in three stages with the onsets about 350, 440 and 530 K. Note that our previous studies of other Mn-doped $YAlO_3$ crystals in similar experimental conditions [6] revealed two dominant stages of bleaching of the induced absorption: starting from about 350 and 520 K.

The three stages of bleaching of the induced absorption (starting from 350, 440 and 530 K) can be correlated with the three main TL peaks observed in the present study at 400, 450 and 560 K. The absorption induced in the oxidized crystal is completely removed already after the first two stages of warming up (see figure 9). This is in agreement with the increased intensity

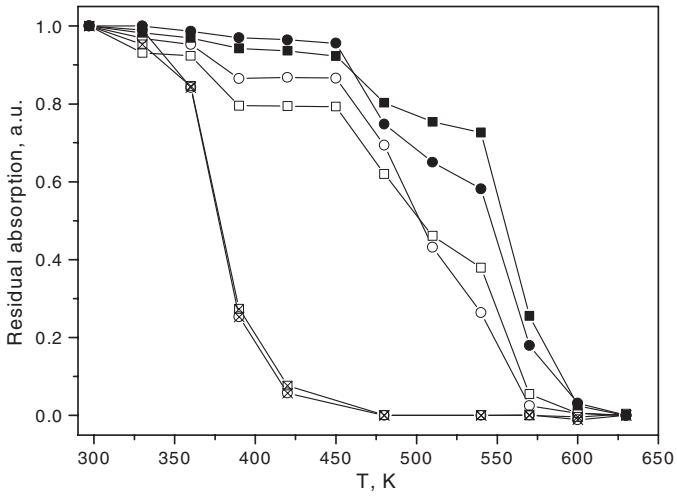

Figure 9. Discolouration kinetics registered at 15 000 cm^{-1} (circles) and 18 000 cm^{-1} (squares) for the laser illuminated $YAlO_3$:Mn(0.2%) crystals: (i) as grown (open symbols), (ii) annealed in air (crossed symbols) and (iii) annealed in hydrogen (solid symbols).

of the first two TL emission peaks and the decreased intensity of the third TL peak of the crystal (see figure 5). On the other hand, a much weaker bleaching of the absorption after the first two warming up stages is observed for the crystal annealed in hydrogen. This coincides with the decreased intensity of the first two TL peaks of the crystal in comparison with the as-grown crystal.

The above correlation means that the decay of the Mn^{5+} absorption bands, due to recombination of electrons released from deep traps ($Mn^{5+} + e^- \rightarrow Mn^{4+}$), is accompanied by the red TL emission of Mn^{4+} ions.

3.4. Colouration and discolouration processes after γ-irradiation

The additional absorption spectra of $YAlO_3$:Mn crystals after γ-irradiation are presented in figure 10. As shown previously [6], ionizing irradiation induces the same ionization of Mn^{4+} ions as the laser illumination as well as some additional recharging processes, which involve Mn^{2+} ions and are visible in the additional colouration of the crystals due to a wide absorption band centred at about 26 000 cm^{-1}.

The x-ray luminescence spectra (figure 11) demonstrate that γ-irradiation induces a reduction of both the red and yellow–green emission, whereas the laser illumination reduces the red emission only.

The discolouration kinetics registered during warming up of the γ-irradiated crystals are presented in figure 12. The discolouration kinetics registered for the Mn^{5+} absorption bands (15 000 and 18 000 cm^{-1}) for the as-grown and oxidized crystals correlate with the observed red TL emission in a similar manner as for laser illumination. On the other hand, the bleaching of the induced absorption at 26 000 cm^{-1} correlates with the yellow–green TL emission of Mn^{2+} ions.

Very interesting peculiarities have been revealed for the crystal annealed in hydrogen. Namely, some new absorption bands appeared during warming up of the γ-irradiated crystal (see figure 13). The absorption bands are centred at 7500, 18 200, 19 800 and 22 000 cm^{-1}. As can be seen in figure 14, all these absorption bands start to grow above 420 K. Moreover, the

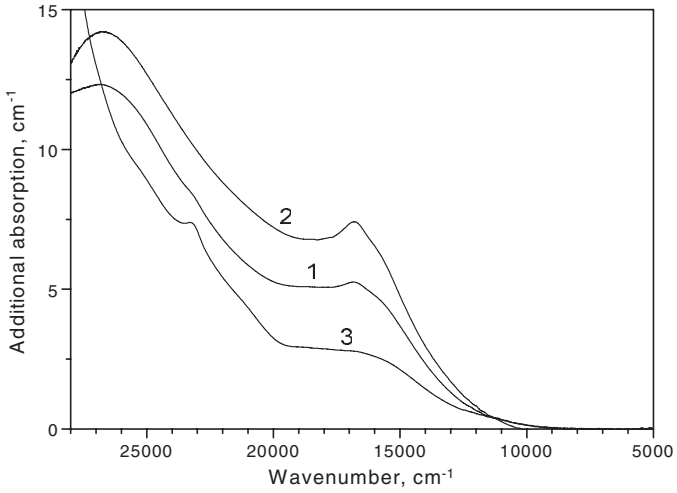

Figure 10. Additional absorption spectra of the $YAlO_3$:Mn(0.2%) crystals after γ-irradiation (dose of 10 kGy): 1—as-grown crystal; 2—crystal annealed in air; 3—crystal annealed in hydrogen.

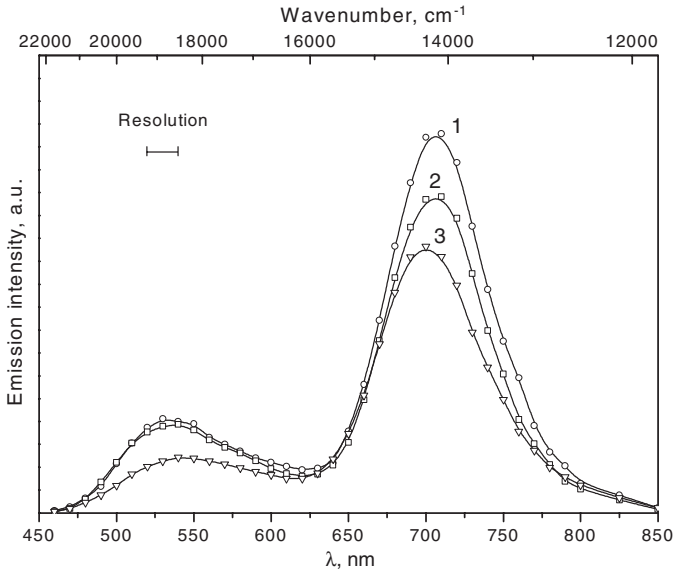

Figure 11. X-ray luminescence spectra of the as-grown $YAlO_3$:Mn(0.2%) crystal: 1—not exposed; 2—laser illuminated ($\lambda = 514.5$ nm); 3—γ irradiated (dose 1 kGy).

band at 18 200 cm^{-1} fully disappears above 630 K. The bands at 7500, 19 800 and 22 000 cm^{-1}, on the other hand, disappear only after warming up above 800 K, when the crystal's colouration returns to the previous, unexposed state. The discolouration kinetics of the bands at 7500 and 22 000 cm^{-1} are similar to that of the 19 800 cm^{-1} absorption band presented in figure 14.

The $YAlO_3$:Mn crystal in the intermediate state of colouration, corresponding to line 4 in figure 13, reveals a characteristic photoluminescence spectrum at Ar^+-laser excitation (see figure 15). The Ar^+-laser line ($\lambda = 514.5$ nm) used for excitation coincides with the newly formed absorption band at 19 800 cm^{-1}. The photoluminescence spectrum of Mn^{4+} ions is

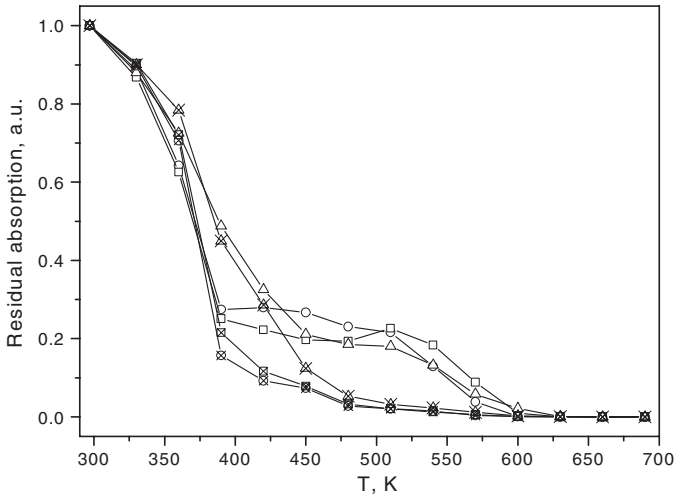

Figure 12. Discolouration kinetics registered at 15 000 cm^{-1} (circles), 18 000 cm^{-1} (squares) and 26 000 cm^{-1} (triangles) for the γ-irradiated (dose of 10 kGy) $YAlO_3$:Mn(0.2%) crystals: (i) as-grown crystal (open symbols) and (ii) crystal annealed in air (crossed symbols).

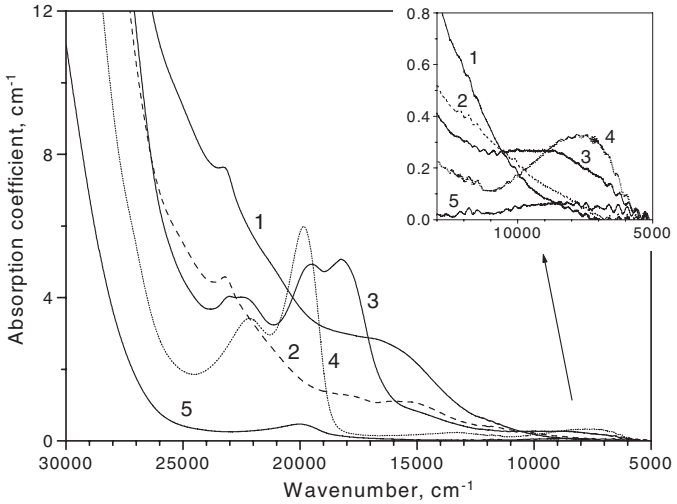

Figure 13. Optical absorption spectra of the $YAlO_3$:Mn(0.2%) crystal annealed in hydrogen after γ-irradiation (dose of 10 kGy) at room temperature (1) and after a number of subsequent warming processes at $T = 420$ K (2), $T = 510$ K (3), 720 K (4) and $T = 810$ K (5).

superimposed on a wide band extending from 570 to about 1000 nm at room temperature. This band is similar to the luminescence spectrum of Mn^{3+} ions in octahedral coordination observed in garnet crystals [13]. The Mn^{3+} ($3d^4$) ions in garnets give the absorption band near 20 000 cm^{-1} ($^5E \rightarrow {}^5T_2$ transition) as well as the band near 7500 cm^{-1} (transition between two Jahn–Teller split components of the ^5E ground state) [13]. In view of such similarity it seems probable that the newly formed absorption bands at 7500 and 19 800 cm^{-1} observed by us belong to the Mn^{3+} ions created in place of Mn^{4+} ions.

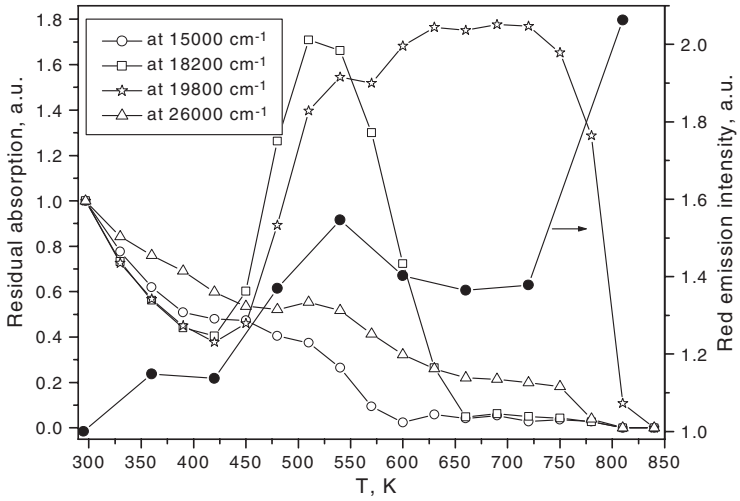

Figure 14. Discolouration kinetics for the γ-irradiated (dose of 10 kGy) $YAlO_3$:Mn(0.2%) crystal previously annealed in hydrogen. Solid circles represent the red emission intensity of the crystal under x-ray excitation.

Our measurements of x-ray luminescence confirm this supposition. By analogy with the discolouration kinetics registered at a certain wavelength, we have measured the x-ray luminescence spectra and their modification after warming up of the γ-irradiated crystals, especially the crystal previously annealed in hydrogen. The temperature dependence of the emission intensity at 710 nm under x-ray excitation, which we associate with the Mn^{4+} ions, is shown in figure 14. The γ-irradiation of the crystal up to a dose of 10 kGy results in a decrease of the red emission near 710 nm by a factor of about 2.1. Subsequent warming up of the crystal leads to an increase of the red emission that correlates with the bleaching of the Mn^{5+} absorption at 15 000 cm^{-1}. Unlike the as-grown or air annealed crystals, for which the red emission was restored to the initial level right away after the induced absorption of Mn^{5+} ions disappeared (above 600 K), in the case of the hydrogen annealed crystal the red emission does not return to the previous level even after the Mn^{5+} absorption is completely removed (see figure 14). Moreover, the red emission decreases slightly above 550 K, which correlates with the rise of the absorption band at 19 800 cm^{-1}. The red emission is completely restored to the previous level only after the 19 800 cm^{-1} absorption band is bleached, which occurs above 750 K. Thus, the red emission of the crystal in the intermediate state of colouration (corresponding to line 4 in figure 13) is lower by a factor of 1.5 relative to the non-irradiated state (line 5 in figure 13). This indicates that a fraction of the Mn ions is in the 3+ instead of 4+ charge state.

It should be emphasized that Mn^{3+} ions are formed only in the crystals annealed in hydrogen as an intermediate stage during warming up of the γ-irradiated crystals. They are absent in the crystals after the hydrogen annealing (without any irradiation) as well as in the crystals just after γ-irradiation (without subsequent warming up), as confirmed by the absorption and luminescence measurements presented above.

The changes of the yellow–green emission during warming up of the γ-irradiated crystal previously annealed in hydrogen are difficult to interpret because of strong reabsorption in this spectral region caused by the newly formed absorption bands at 18 200, 19 800 and 22 000 cm^{-1}.

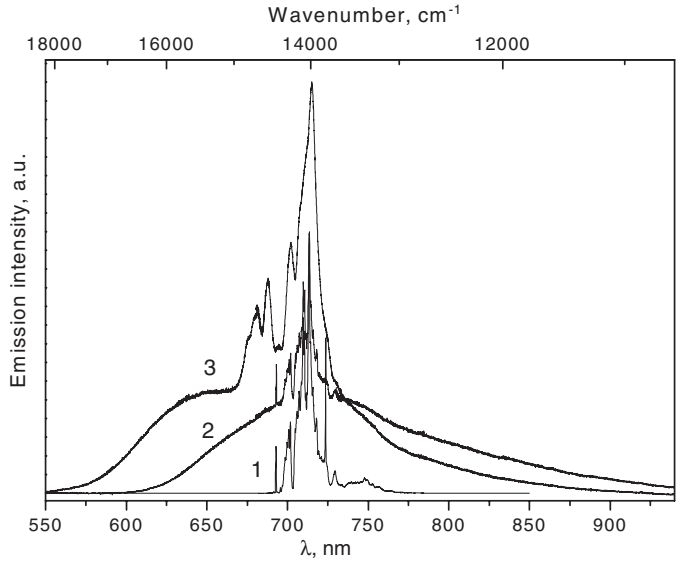

Figure 15. Photoluminescence spectra of the $YAlO_3$:Mn(0.2%) crystal annealed in hydrogen (1) and after that γ irradiated and warmed up to $T = 720$ K (that corresponds to curve 4 in figure 13) (2, 3). The spectra were recorded at $T = 10$ K (1, 2) and $T = 300$ K (3) under Ar^+-laser excitation ($\lambda = 514.5$ nm).

4. Conclusions

With use of optical spectroscopy techniques we confirmed the presence of both Mn^{4+} and Mn^{5+} ions in Al positions, as well as Mn^{2+} ions in Y positions in the as-grown $YAlO_3$:Mn crystals.

The high-temperature annealing ($T = 1300$ K) of the as-grown $YAlO_3$:Mn crystals in reducing atmosphere (hydrogen) removes almost completely the Mn^{5+} ions due to the $Mn^{5+} \rightarrow Mn^{4+}$ reaction, that is charge compensated apparently by the loss of oxygen from the crystal.

The high-temperature annealing of the crystals in oxidizing atmosphere (in air) has an inverse effect. Such annealing increases the number of Mn^{5+} ions due to the $Mn^{4+} \rightarrow Mn^{5+}$ oxidation process.

Silicon co-doping of the crystals practically does not change the number of Mn^{2+} ions and reduces the number of Mn^{4+} ions by a half. Owing to the small ionic radius of Si^{4+} ions we assume that they occupy Al positions in the host and so prevent Mn^{4+} ions entering these positions.

The Mn^{4+}-related TL emission in the first two peaks (at 400 and 450 K) is strongly reduced in crystals annealed in hydrogen in comparison with the as-grown crystals both after laser ($\lambda = 514.5$ nm) and γ-irradiation. This is correlated with the smaller intensity of photocolouration (caused by Mn^{5+} ions) of the crystals. On the other hand, the red TL emission in the first two peaks of the crystals previously annealed in air increases strongly both after laser and γ-irradiation.

As regards the Mn^{2+}-related TL emission induced by γ-irradiation, air annealing leads to a decrease of this yellow–green TL emission in comparison with the as-grown crystals. Hydrogen annealing leads to an increase of the integral intensity of the TL emission mainly due to the drastic growth of the peak at 380 K.

An interesting peculiarity of the hydrogen annealed crystals was observed at warming up of the γ-irradiated crystals. Some new absorption bands (at 7500, 18 200, 19 800 and 22 000 cm^{-1}) arose after warming up above 420 K. The band at 18 200 cm^{-1} was fully bleached above 630 K, whereas the bands at 7500, 19 800 and 22 000 cm^{-1} disappeared only above 750 K. The newly formed absorption bands, at least at 7500 and 19 800 cm^{-1}, were attributed to Mn^{3+} ions, which are created in place of Mn^{4+} ions.

Acknowledgments

The work was partially supported by the Ukrainian Ministry of Education and Science (project No 0104U002301, acronym Cation) and by the grant of the Polish Committee for Scientific Research during years 2006–2009.

References

[1] Loutts G B, Warren M, Taylor L, Rakhimov R R, Ries H R, Miller G, Noginov M A, Curley M, Noginova N, Kukhtarev N, Caulfield H J and Venkateswarlu P 1998 *Phys. Rev.* B **57** 3706
[2] Noginov M A, Noginova N, Curley M, Kukhtarev N, Caulfield H J, Venkateswarlu P and Loutts G B 1998 *J. Opt. Soc. Am.* B **15** 1463
[3] Kukhtarev N and Kukhtareva T 2003 *Opt. Mem. Neural Netw.* **12** 75
[4] Zhydachevskii Ya, Durygin A, Suchocki A, Matkovskii A, Sugak D, Bilski P and Warchol S 2005 *Nucl. Instrum. Methods Phys. Res.* B **227** 545
[5] Rakhimov R R, Wilkerson A L, Loutts G B, Noginov M A, Noginova N, Lindsay W and Ries H R 1998 *Solid State Commun.* **108** 549
[6] Zhydachevskii Ya, Durygin A, Suchocki A, Matkovskii A, Sugak D, Loutts G B and Noginov M A 2004 *J. Lumin.* **109** 39
[7] Li G, Guo X, Lu J, Shi Z, Wu J, Chen Y and Chen J 1992 *J. Cryst. Growth* **118** 371
[8] Shannon R D 1976 *Acta Crystallogr.* A **32** 751
[9] Noginov M A and Loutts G B 1999 *J. Opt. Soc. Am.* B **16** 3
[10] Noginov M A, Loutts G B, Noginova N, Hurling S and Kück S 2000 *Phys. Rev.* B **61** 1884
[11] Zhydachevskii Ya, Suchocki A, Zakharko Ya and Berkowski M 2006 Photoluminescence studies of Mn^{4+} ions in $YAlO_3$, in preparation
[12] Zhydachevskii Ya, Durygin A, Suchocki A, Matkovskii A, Sugak D and Frukacz Z 2004 *Phys. Status Solidi* c **1** 312
[13] Kück S, Hartung S, Hurling S, Petermann K and Huber G 1998 *Phys. Rev.* B **57** 2203